# EVALUATING BASALT FABRIC IN STUFFED WHIPPLE AND MULTISHOCK SHIELDS THROUGH COMPARATIVE HYPERVELOCITY TESTS


**Christopher J. Cline II(1), Bruce Alan Davis(2), Jesus Resendez(2), Trevor Aston(2)**

*(1) NASA Johnson Space Center, Astromaterials Research and Exploration Science, Mail code X15, 2101 NASA Parkway, Houston, TX 77058, United States), Email: christopher.j.cline@nasa.gov*

*(2) Amentum, NASA Johnson Space Center, Astromaterials Research and Exploration Science, 2101 NASA Parkway Houston, TX 77058, United States), Email: bruce.davis-1@nasa.gov, jesus.h.resendez@nasa.gov*

*(3) Aerodyne, NASA Johnson Space Center, Astromaterials Research and Exploration Science, 2101 NASA Parkway Houston, TX 77058, United States), Email: trevor.c.aston@nasa.gov*



## ABSTRACT

Soft goods are often used in micrometeoroid and orbital debris (MMOD) shields as means to provide targeted material properties with a relatively low areal density. In this study, basalt fabric (glass fiber made from melting volcanic rocks) is substituted for Nextel™ in two widely used MMOD shields, the multi-shock and stuffed Whipple designs. Hypervelocity testing was conducted using scaled-down versions of these two shields, and the ultimate performance (pass or fail) was compared to the predictions of the original ballistic limit equations that were derived using Nextel™ to determine if the equations can properly parametrize the basalt fabric without additional equation modification. Multi-shock shields showed comparative performance between the two different fabrics with no deviations from the prediction of performance from the ballistic limit equation (BLE) to actual observed performance. Testing on the stuffed Whipple design, however, showed conflicting results depending on the geometric scale of the tests, thus preventing a robust conclusion on the relative performance of basalt fabric in comparison to Nextel™, but suggests that the equation would still be appropriate for use with either ballistic fabric.


## 1 INTRODUCTION

Ballistic fabrics have been an integral part of micrometeoroid and orbital debris (MMOD) shields for over three decades. These materials offer a unique flexibility not only in offering tuneable material properties that can provide targeted enhancements to specific shield functions (i.e., projectile disruption/comminution, or arresting debris cloud momentum), but also tangible and physical flexibility, which provides an immediate advantage relating to the practicability of mounting these shields on flight hardware. With each part of a MMOD shield requiring distinctive properties to optimize its performance, a variety of ballistic fabrics have become mainstays [1]. The capabilities of a bumper (or thin sacrificial layer near the space-facing side of a MMOD shield) for example, relies mainly on density and having enough thickness to produce a shock wave that is wide enough to completely shock an incoming projectile. For this purpose, silica-fiberglass-, or ceramic-based fabrics, generally have higher density fibers that have been shown to provide excellent projectile disruption capabilities. The selection of a material for the portion of the MMOD shield closer to the rear wall, in comparison, needs to consider the tensile strength of the fabric, since this is where a broader footprint of the laterally expanding debris cloud will impact and induce a substantial impulse load onto the shield. Traditionally, materials such as Kevlar® (usually employed for slower speed ballistic and stab/cut protection) offer ideal properties for this purpose.

Through the process of a MMOD risk analysis, a user must have a quantified measure of the ballistic performance for all MMOD shields used on a spacecraft, which is provided by selecting appropriate ballistic limit equations (BLEs) that define the particle size that would "fail" the shield as a function of projectile type, impact speed, impact angle, and any other pertinent impact or shield parameters. In an ideal situation, every MMOD shield configuration on a spacecraft would have a dedicated hypervelocity testing campaign to interrogate the performance of the MMOD shields for the development of specific BLEs. In reality, however, and often due to financial and schedule constraints, BLEs are often assigned/adopted/modified to fit a specific MMOD shield configuration using a combination of educated engineering judgments and a bevy of historic hypervelocity testing data. The delineation as to when this original BLE is no longer directly applicable to the new MMOD shield design, albeit through its geometry and/or choice of materials, is nuanced, and often left up to individual analyst.

In the absence of a specific flight program to drive testing of new materials used in MMOD shields, research can still be conducted to interrogate performance of existing BLEs, and specifically the applicability of their inputs to appropriately parametrize new materials in the calculation of a critical particle diameter. Such efforts thus expand the ever-important hypervelocity impact data set that is leveraged when selecting initial BLEs. To this end, here, hypervelocity testing is conducted using


*Proc. 9th European Conference on Space Debris, Bonn, Germany, 1–4 April 2025, published by the ESA Space Debris Office*
*Editors: S. Lemmens, T. Flohrer & F. Schmitz, (http://conference.sdo.esoc.esa.int, April 2025)*

basalt fabric in two common MMOD shields that contain ballistic fabric, as the original data sets used to constrain the respective BLEs did not utilize this material.

## 2 METHODOLOGY

### 2.1 MMOD Shield designs

Two main MMOD shield designs are used for this study on the performance of basalt fabric in hypervelocity impacts, the multi-shock and stuffed Whipple. Basalt is a common igneous rock that has high concentrations of Fe and Mg. This rock is melted and spun into a fiber, and due to the composition, yields a relatively high-density fabric that may perform well as a projectile disruptor layer. The first MMOD shield variant that will be tested is the multi-shock shield [2]. This shield has typically been made from multiple layers of Nextel™ each mounted with an interstitial gap, and here these layers will be substituted with basalt to test the applicability of the BLE inputs to predict the ballistic performance. Second, the stuffed Whipple shield [3] will be used. This shield often appears as a standard metallic Whipple shield [4] but contains a layer of soft-goods halfway between the metallic plates that contains Nextel™ on the space-facing side, followed by Kevlar® facing the rear wall. Variants will substitute basalt, again, for Nextel™.

Due to costs of testing full-scale module-sized shields (larger shield = larger particle required to reach shield failure = larger gun need to launch projectile) all components of the shields have been geometrically scaled down, including the bumper and rearwall thickness and stuffing areal density. At the beginning of this study, all shields were scaled so that the predicted critical particle diameter could be obtained by using the .17-caliber two-stage light-gas gun, capable of launching a saboted Al projectile up to ~3.2 mm in diameter. It will be shown in later sections, however, that a portion of testing on the stuffed Whipple design employed a second geometric scaling for an internal comparison to examining any unwanted artifacts from geometric scaling. It is also important to note that the areal density of the different variants of each MMOD shield type was kept as consistent as practical when switching ballistic fabrics. This is important since the areal density of the shield, or stuffing, are main inputs in the relevant BLEs. While great strides were made to keep the areal density exact, some experimental deviation was unavoidable, but in all cases, except for one test, were kept to <1%.

The multi-shock shield contained four layers of ballistic fabric, followed by a single aluminum rearwall. A picture taken normal to the projectile trajectory, and accompanying 3D illustration of the shield is provided in Fig. 1. Two variants of this shield were tested, one where all fabric layers were composed of Nextel™, and a second where all layers were composed of basalt fabric. Table 1 details the exact construction of each test, and it can be seen that two different variations of the basalt construction were tested to achieve the same total areal density as the Nextel™ variant – one where the bulk of the basalt mass was placed at the front of the shield, and another where the bulk of the mass was closer to the rearwall. This choice was intentional to determine if either of these designs provided superior performance over the other.

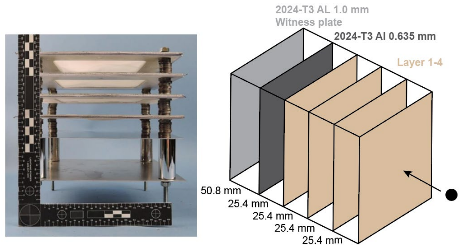


*Figure 1. Photograph of multi-shock shield taken normal to the projectile trajectory (left), and a 3D representation of the shield (right). Layers 1-4 for each test are defined in Table1.*

The stuffed Whipple shield is defined by a metallic bumper and rearwall with the addition of "stuffing" set halfway between these two plates. Two different size-scales of this general shield design were tested in this study, one where the total standoff distance between the bumper and rearwall was only 28.6 mm, and another where the total standoff distance was 85.8 mm (Figs. 2 and 3). These shields represent an approximate ¼- and ¾-scale variant of the shielding on the US module of the ISS, and similar hypervelocity impact studies routinely use scaled-down designs to probe general shield behavior (e.g., ref [5]). For the ¼-scale tests articles, three variants were tested – one that mimics the materials of the ISS shields (stuffing includes Nextel™ AF-10 + Kevlar® 775), another that substitutes basalt for the Nextel™, and finally one that uses a combination of basalt and the newest generation Kevlar® called EXO™ 1100[6]. Testing the newest generation of Kevlar was also used to compare the performance of the heritage shield design with this updated material. For the ¾-scaled test articles, the standard ISS shield was first tested, then two others were tested using the Kevlar® EXO™ 1100, one with Nextel™ AF-10 disruptor, and another with basalt. All tested configurations are listed in Table 1.

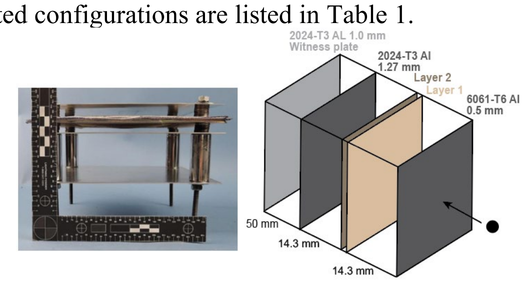


*Figure 2. Photograph of ¼-scale stuffed Whipple shield taken normal to the projectile trajectory (left), and a 3D representation of the shield (right). Layers 1and 2 for each test are defined in Table1.*

**Table 1**. Tested configurations

| Test number | Al-6061 bumper (mm) | Layer 1 (g/cm$^2$) | Layer 2 (g/cm$^2$) | Layer 3 (g/cm$^2$) | Layer 4 (g/cm$^2$) | Al-2024 Rear wall (mm) | Total areal density (g/cm$^2$) |
|---|---|---|---|---|---|---|---|
| **Multi-shock** | | | | | | | |
| 24239 | - | Nextel AF-10 (0.029) | Nextel AF-10 (0.029) | Nextel AF-10 (0.029) | Nextel AF-10 (0.029) | 0.635 | 0.287 |
| 24240 | - | Basalt (0.040) | Basalt (0.036) | Basalt (0.020) | Basalt (0.020) | 0.635 | 0.287 |
| 24241 | - | Basalt (0.020) | Basalt (0.020) | Basalt (0.036) | Basalt (0.040) | 0.635 | 0.287 |
| 24242 | Same as test 24241 | | | | | | |
| **1/4-scale Stuffed Whipple** | | | | | | | |
| 24235 | 0.5 | Nextel AF-10 (0.146) | Kevlar 775 (0.046) | - | - | 1.27 | 0.683 |
| 24236 | Same as test 24235 | | | | | | |
| 24238 | Same as test 24235 | | | | | | |
| 24261 | Same as test 24235 | | | | | | |
| 24237 | 0.5 | Basalt (0.148) | Kevlar 775 (0.046) | - | - | 1.27 | 0.685 |
| 24243 | 0.5 | Basalt (0.080) | Kevlar EXO (0.115) | - | - | 1.27 | 0.686 |
| 24244 | Same as test 24243 | | | | | | |
| 24262 | Same as test 24243 | | | | | | |
| **3/4-scale Stuffed Whipple** | | | | | | | |
| 24263 | 1.5 | Nextel AF-10 (0.438) | Kevlar 775 (0.138) | - | - | 3.81 | 2.049 |
| 24265 | 1.5 | Same as test 24263 | | | | | |
| 24264 | 1.5 | Basalt (0.240) | Kevlar EXO (0.345) | - | - | 3.81 | 2.058 |
| 24266 | 1.5 | Same as test 24264 | | | | | |
| 24282 | 1.5 | Nextel AF-10 (0.438) | Kevlar EXO (0.345) | - | - | 3.81 | 2.256 |

Standoff of each layer: Multi-shock = 2.54 mm, ¼-scale stuffed Whipple = 14.3 mm, ¾-scale stuffed Whipple = 42.9 mm

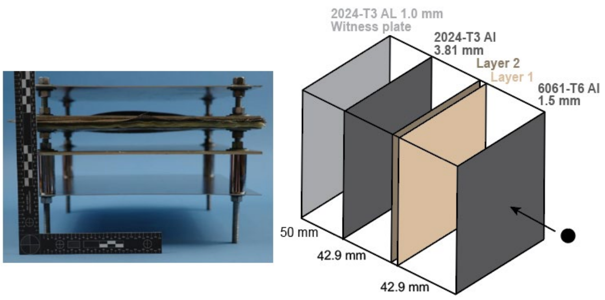


*Figure 3. Photograph of ¾-scale stuffed Whipple shield taken normal to the projectile trajectory (left), and a 3D representation of the shield (right). Layers 1and 2 for each test are defined in Table1.*

### 2.2 Hypervelocity testing

In total, 17 hypervelocity tests were conducted as part of this study on the relative performance of MMOD shields constructed with basalt fabric. All tests were conducted at the Remote Hypervelocity Test Laboratory at NASA White Sands Test facility using either .17-caliber or .50-caliber two-stage light-gas gun. Spherical Al 2017-T4 projectiles were used in every test, with the diameter varying for the specific configuration. Impact velocities were nominally kept at 7.0 km/s (± experimental variability in conducting hypervelocity tests) and values are reported in Table 2 that were determined by means of laser occultation to a precision within 0.05 km/s.

### 2.3 Damage characterization

After hypervelocity testing, each article is photographed as a whole, and then dissembled. Layers of interest are then imaged using high-resolution photography and/or captured by 3D-scanning using a Keyence VR-5200 with a spatial resolution of 4 μm. Damage dimensions are then recorded as the maximum magnitude observable and a second measurement is taken in a direction normal to the first orientation.

## 3 DATA

### 3.1 Experimental summary

Details of the three main shield types/scales are provided in the following section. Results are presented as in three sections, starting with the results from the multi-shock shield, followed by the ¼-scale stuffed Whipple, then the ¾-sale stuffed Whipple. A table summary of the testing conditions (velocity and projectile size) and results of the tests are provided in Table 2. For the purpose of this study, failure is defined as threshold perforation of the metallic rear wall for any shield configuration. Given the discrete sizes of projectiles available, in combination with the constrained number of tests, fully bracketing the pass/fail performance of all tested configurations was not feasible. In these instances, the magnitude of damage sustained to the rearwall or witness plate, is used to inform the relative performance of the shield for comparative purposes.

### 3.2 The multi-shock shield

Only a single baseline test of the Nextel™ multi-shock shield was tested in this study. An additional four data points for this design are detailed in ref [7] that used the exact geometry of this shield. Despite the additional data, there was no discernible difference in relative pass/fail performance between the multi-shock shield constructed of Nextel™ or basalt.

A close examination of the damage sustained to the rearwalls for a few select tests (shown in Fig. 4) does indicate a possible difference in projectile breakup. For a 2.8 mm Al projectile, the rearwall for the basalt shield produced a smooth, low-slope bump on the rearwall. The Nextel™ shield, in contrast, exhibited multiple small bumps superimposed on a larger deflection of the rearwall. Presence of these bumps suggests that for this given projectile size, the Nextel™ allowed solid fragments to persevere through the shield and impact the rearwall, where the basalt shows no such indications. Despite these small differences, all shields, irrespective of materials or construction method, passed when impacted by a 2.88 mm Al projectile, and failed when impacted with a 2.99 mm, or larger, Al projectile – effectively bracketing the ballistic limit equation at ~7.0 km/s between these particle diameters.


*Figure 4. Post-test photographs of the backside of the rearwall from the three variants of the multi-shock shield (label in bottom left, projectile size in parenthesis). Oblique views of damage provided as insets.*

**Table 2**. Test matrix

| Test number | Projectile diameter (mm) | V (km/s) | Pass/fail | Damage characterization |
|---|---|---|---|---|
| **Multi-shock** | | | | |
| 24239 | 2.80 | 7.05 | Pass | Bump formed on RW with maximum deflection of ~2.5 mm. Multiple dimples appear on bump. |
| 24240 | 2.99 | 6.86 | Fail | 11.9 x 8.7 mm irregularly shaped perforation of RW (tearing). WP exhibits a few small bumps. |
| 24241 | 2.80 | 6.91 | Pass | Deflection of RW has a low slope and max magnitude of 3.5 mm. |
| 24242 | 2.99 | 6.98 | Fail | 13.3 x 9.8 mm perforation in RW. Minor surface pitting on WP. |
| **1/4-scale Stuffed Whipple** | | | | |
| 24235 | 2.50 | 6.87 | Pass | Material deposition and pitting on RW, with max deflection of 1.7 mm. |
| 24236 | 2.71 | 6.86 | Pass | Pitting and cratering on RW, sharp bump formed with a max deflection of 3.2 mm. |
| 24238 | 2.80 | 7.14 | Pass | Pitting and cratering on RW, sharp bump formed with a max deflection of 3.2 mm. |
| 24261 | 3.0 | 7.08 | Pass | Sharp peak on RW bump, max deflection 4.6 mm. Possible incipient tear forming on peak. |
| 24237 | 2.71 | 7.03 | Fail | Multiple perforations in RW, largest is 7.5 x 5.4 mm, no perceived deflection of RW. |
| 24243 | 2.71 | 6.89 | Pass | Bumper on RW max deflection of 2.0 mm. One additional dimple found on bump. |
| 24244 | 2.80 | 7.04 | Pass | Bumper on RW max deflection of 3.0 mm. |
| 24262 | 3.0 | 7.05 | Pass | Bumper on RW max deflection of 3.5 mm. |
| **3/4-scale Stuffed Whipple** | | | | |
| 24263 | 9.53 | 6.89 | Fail | Large perforation and cracking of RW 17.6 x 16.0 mm. Multiple perforations on WP. |
| 24265 | 8.72 | 6.89 | Fail | 10.62 x 6.77 mm perforation of RW. Only minor pitting on WP, no deflections noted. |
| 24264 | 9.53 | 6.90 | Fail | Large perforation of RW 30.3 x 25.5 mm. |
| 24266 | 8.72 | 6.92 | Pass | Deposition of pitting of RW, maximum deflection of 12.4 mm. |
| 24282 | 8.72 | 6.93 | Fail | RW perforation measuring 9.8 x 10.77 mm. Two bumps on WP, largest is 1.82 mm in deflection. |

*RW=rearwall, WP=witness plate

### 3.3 ¼-scale Stuffed Whipple

Four tests were conducted on the baseline ISS-inspired stuffed Whipple design consisting of Nextel™ AF-10 and Kevlar® with projectiles ranging in diameter from 2.5 and 3.0 mm. None of these tests were able to fail the baseline design (Fig. 5), thus an upper limit of ballistic performance was not determined. Swapping the Nextel for basalt in this design yielded a failure with a 2.71 mm projectile. Further, the rearwall exhibited multiple perforations, suggesting that the baseline Nextel™ design was performing better, and that the basalt fabric was not thoroughly disrupting the projectile.

Further modifications to this design included then swapping the Kevlar®775 that was paired with basalt for Kevlar® EXO™1100. This final design performed as well as the baseline, passing when impacted by a 3.0 mm projectile (Fig. 5). Comparing the deflections of the rearwalls from the basalt + Kevlar® EXO™1100 and baseline shield variants shows variations in total magnitude of deflection. The basalt + Kevlar® EXO™1100 had notably less deformation with a magnitudes of 3.5 mm, compared to the 4.6 mm from the baseline. Due to testing limitations, larger projectiles were not used on the ¼-scale shields to define a particle size that would lead to failure.

### 3.4 ¾-scale stuffed Whipple

Given the inability to fail the two of the ¼-scale stuffed Whipple shields using the smaller .17-caliber gun, testing was moved to the larger .50-caliber range. Such a change offered an opportunity to increase the scaled-size of the shield to simultaneously test the relative performance of basalt, as well as the consistency of testing results at different dimensional scales. Two tests were conducted on the baseline design with 9.53- and 8.72-mm projectiles, but both failed, despite a simple scaling the 1/4-scale results suggesting a pass at these projectile sizes (Fig. 6). With the previous testing showing better performance from the basalt + Kevlar® EXO™1100 design, testing resumed here, which bracketed the pass/fail performance between 8.72- and 9.53-mm, thus outperforming the baseline shield variant (Fig. 6).

The better performance of the basalt + Kevlar® EXO™1100 design could not be directly attributed to the substitution of basalt fabric since the type of Kevlar® also differed between the two designs. To address this additional parameter, a final test was conducted that combined Nextel™ AF-10 and Kevlar® EXO™1100. Due to the materials available, this shield had an areal density that was 10% higher than any other shield tested in this study, but still failed when impacted with an 8.72-mm projectile at 6.93 km/s (Fig.6).

## 4 DISCUSSION

### 4.1 Ballistic performance and BLEs

Comparison of relative ballistic performance for each shield configuration, and their respective construction materials, can be made through both visual examination of the tested articles, and by plotting pass/fail results as a function of particle size against the most relevant ballistic limit equation. The prior technique provides a qualitative assessment of performance when the granularity of the data acquisition may be limited – in such a situation where the ballistic limit of the shield configuration is between two available projectile sizes – where the latter comparison provides an opportunity to probe the parameterization of the BLE to see if the performance of the shield is accurately predicted when using any materials.

Assessing the relative performance of basalt fabric to Nextel™ in a multi-shock shield was limited by the available number of tests. From a pass/fail perspective, and as a function of projectile size defeated for a nominal 7.0 km/s impact, both shield variants were able to resist a 2.8 mm projectile, but the basalt shield failed when impacted by a 2.99 mm projectile (Fig. 4). Examining the post-test samples provides no clear conclusion on which fabric performs better at this scale. The rear wall from the basalt shield showed a smooth broad deflection from the debris cloud impulse load, where the rearwall of the shield constructed of Nextel™, in contrast, showed additional dimples (small craters) on top of this broader deflection. While this finding may suggest that the basalt fabric is performing better as a disrupter layer, the overall magnitude of the deflection from the basalt shield was ~30% larger than that measured on the Nextel™ shield (3.5-mm compared to 2.5-mm), suggesting that the rearwall may be closer to the ballistic limit for this shield.


*Figure 5. Post-test photographs of the backside of the rearwall from the three variants of the ¼-scale stuffed Whipple shield (label in bottom left, projectile size in parenthesis). Oblique views of damage provided as insets.*


*Figure 6. Post-test photographs of the backside of the witness plates from the three variants of the ¾-scale stuffed Whipple shield (label in bottom left, projectile size in parenthesis). Oblique views of damage provided as insets.*

The ballistic limit equation used for this shield is identical to that provided in section 4.5.2 of ref [8]. The testing results included in this contribution are plotted against that BLE along with three supplemental data points from ref [7] that used the same shield geometry, see Fig. 7a. While the BLE requires a scaling factor to fit the experimental data, it is observed that the current BLE equally predicts the performance of shields made with either basalt or Nextel™, suggesting that the inputs into the BLE are appropriately parameterized for inclusion of basalt fabrics.

Examination of the ¼-scale stuffed Whipple shield variants shows a greater disparity in performance between the disrupter layer in the stuffing being made of either basalt or Nextel™ (both paired with Kevlar®775). The baseline Nextel™ + Kevlar® 775 design was able to resist projectile sizes up to 3.0 mm, at which point testing was concluded on this design (Fig. 5). The shield fabricated with a basalt disrupter layer, in contrast, failed when impacted with a 2.71 mm projectile at 7.0 km/s. Post-test examination of this test revealed multiple perforations in the rearwall, suggesting that the basalt layer did not adequately disrupt the Al projectile. Poor projectile breakup from the basalt fabric in the stuffed Whipple is inconsistent with the observations from the multi-shock shields, where it was observed to possibly have superior projectile disruption qualities within the limited data set.

Basalt fabric was then paired with the latest generation of Kevlar® to determine if performance would increase to a level equivalent to that of the baseline shield design. To accommodate the extra areal density associated with Kevlar® EXO™1100, and to keep the areal density as similar as possible to the previous designs, the basalt fabric was paired down to almost half of the original areal density. This final shield variant was able to resist a 3.0 mm Al projectile, similar to the baseline design (Fig. 5). Total deflection of the rear wall for the basalt + Kevlar® EXO™1100 was 3.5 mm in comparison to the 4.6 mm of the baseline design – possibly suggesting a better performance of this combination for the same areal density.

All ¼-scale stuffed Whipple test data is plotted along two variations of the BLE provided in section 4.3.2 of ref [8] (see Fig. 7b). Both curves are scaled relative to the original equation by a factor provided in the figure legend, but the relative performance of the shield variants can still be observed. A scaling factor of 0.82 was required to fit the equation to the single failed data point of the basalt + Kevlar ®775 variant. It is important to note that this curve should likely be shifted to even lower scaling factors, but that extent is not fully defined since there was no bracketing test to provide a projectile size that would result in a "pass".

The other two stuffed Whipple variants, however, are antithetical, where only passes were observed, and thus no upper-bound on the critical particle diameter at 7.0 km/s could be determined. A curve was fit directly above the largest projectile size that resulted in a "pass". This decision, at least for the baseline, was justified due to the large deflection of the rearwall suggesting that the shield was close to the ballistic limit. Results from this ¼-scale test series suggested that basalt performs comparatively worse than Nextel™ but can perform as well as the baseline design when paired with Kevlar® EXO™1100.

Careful examination of the rearwalls from the ¼-scale post-test articles indicated that the performance of the Kevlar® may be hampered by the relatively small-scale of the test geometry. Non-dimensional scaling would suggest that if all length-scales of the shield were altered either by the same quantity, that performance should reflect these changes agnostic to the overall shield size. In practicality, however, the standoff distance relative to the size of the fabric weave was not able to be changed, and if the stopping ability of Kevlar®, or basalt, is at all influenced by the length-scale of the weave, then the smaller standoff may be skewing the results of the final "pass/fail" result. Further, the rupture style of the rearwalls were indicating of a possible inability for the Kevlar to fully absorb the impulse load of the debris cloud reaching the rearwall – largely driven by the short standoff. To this end a final test series was designed to scrutinize the comparison of ballistic performance of the baseline design and the well-performing basalt + Kevlar® EXO™1100 at the larger ¾-scale.

Results from testing the ¾-scale stuffed Whipple shield are not wholistically in agreement with the results from the smaller ¼-scale shields. Nondimensional scaling would suggest that the ¾-scale baseline design could resist impact from a 9.0-mm projectile, but failure was observed for both 9.53- and 8.72-mm projectiles, at which point testing was suspended (Fig.6). Testing of the better-performing ¼-scale basalt shield (used in combination with Kevlar® EXO™1100) resulted in a pass at 8.72-mm but resulted in a failure for a 9.53-mm projectile, thus bracketing the BLE within the region of critical particle diameters that would be expected for geometric scaling. Even when failed by the 9.53-mm projectile, the relative damage observed on the witness plate between this test and the Nextel™ baseline indicates better performance from the basalt variant – one in which the number and size of the perforations is noticeably reduced (see Fig. 6) – a result that is counter to the findings of the ¼-scale stuffed Whipple testing. The performance of these two shield variants is plotted against the stuffed Whipple BLE in Fig. 7c, and the necessary scaling factor to derate the performance of the Nextel™ shield is larger in magnitude than what is required to fit the performance of the basalt variant.

Facilitating a direct comparison between the basalt and Nextel™ requires eliminating the non-common components from these variants (i.e. the new Kevlar® EXO™1100), so one final test was conducted where Nextel™ was paired with Kevlar® EXO™1100. Despite the extra mass (areal density), this shield failed when impacted with a 8.72-mm projectile – again suggesting that the basalt fabric disrupter layer in the stuffed Whipple shield outperforms similar shields where the disrupter layer is composed of Nextel™. A BLE for this single data point is not included in Fig 7c due to the much larger variation in areal density.

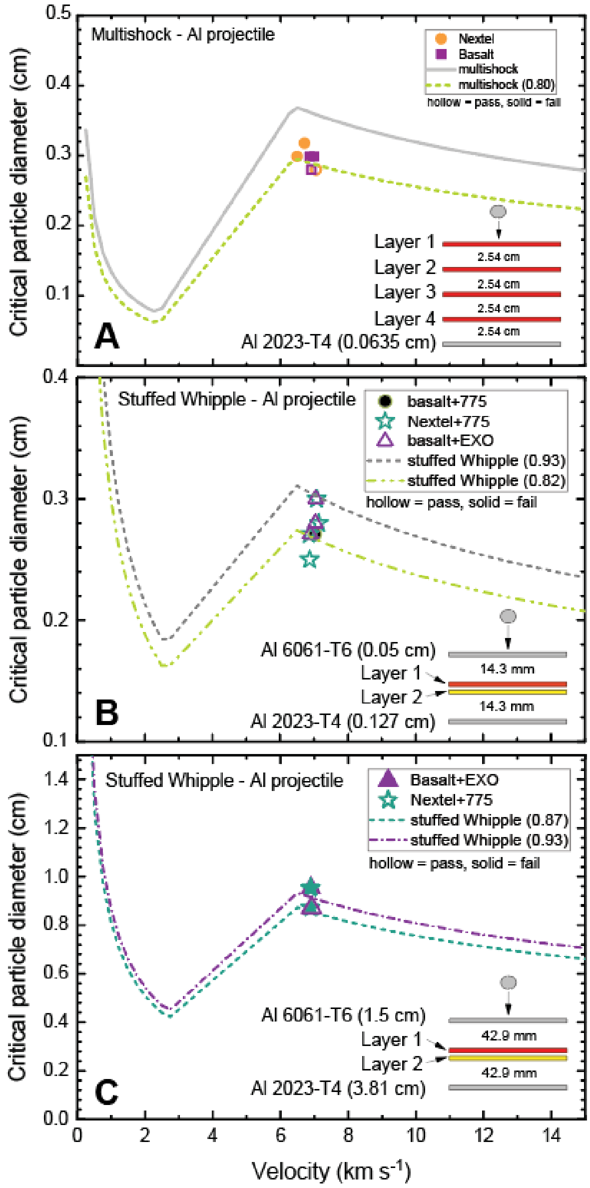


*Figure 7. Ballistic limit equations plotted for the three tested shield configurations. (A) multi-shock, (B) ¼-scale stuffed Whipple, and (C) ¾-scale stuffed Whipple. Layers for each test are defined in Table 1. Parenthetical numbers in legend are scaling factors applied to BLEs.*

## 5 CONCLUSIONS

Here, a study was conducted to examine the relative performance of basalt fabric as a disruptor layer in common varieties of MMOD shields. This was accomplished by conducting a series of hypervelocity impact tests on two well-known MMOD shield types (multi-shock and stuffed Whipple) where basalt fabric was substituted into the design for Nextel™ AF-10. To minimize the influence of variable impact parameters on the comparison these tests were all conducted with Al projectiles launched nominally at 7.0 km/s (± experimental error). Initial testing was conducted on scaled-down versions of these MMOD shields, with total standoffs being on the order of 10 cm for the multi-shock, and only 3 cm for the stuffed Whipple. The results of these tests suggested that the performance of basalt was either comparative to that of Nextel™ (for the multi-shock), or possible worse (for the stuffed Whipple). Physical observations of the post-test shields hinted that the small scale of the stuffed Whipple test articles may be influencing the findings, so additional tests were conducted on larger ¾-scale version of the same stuffed Whipple designs. In contrast to the findings of the ¼-scale experiments, testing of the larger scale shields demonstrated that basalt outperformed shields constructed with Nextel™, regardless of the Kevlar® variant used in the shield. While not unreservedly convincing that one material performs better than another, this test series provide gross confidence in the ability of the current parameterization of the respective BLEs to predict the performance of the shield variants. Simultaneously, however, also highlighting that small differences in predicted critical particles diameters are to be expected, and conducting hypervelocity testing on any shield variant that was not used in the development of the original BLE is always encouraged. The results of this study will now be fed into a larger test campaign being undertaken by the Hypervelocity Impact Technology group to update several BLEs to incorporate a wider range of materials.

## 6 TRADEMARK STATEMENT

Trade names and trademarks are used in this report for identification only. Their usage does not constitute an official endorsement, either expressed or implied, by the National Aeronautics and Space Administration.

## 7 REFERENCES

1. Christiansen, E. L. and D. M. Lear (2015). "Toughened thermal blanket for micrometeoroid and orbital debris protection." Procedia engineering **103**: 73-80.

2. Cour-Palais, B. G. and J. L. Crews (1990). "A multi-shock concept for spacecraft shielding." International Journal of Impact Engineering **10**(1-4): 135-146.

3. Christiansen, E., et al. (1995). "Enhanced meteoroid and orbital debris shielding." International Journal of Impact Engineering **17**(1-3): 217-228.

4. Whipple, F. L. (1947). "Meteorites and space travel." The Astronomical Journal **52**: 131.

5. Christiansen, E. L., et al. (2023). Alternative MMOD Shielding Concepts. Second International Orbital Debris Conference. Houston, TX, 4-7 December.

6. Seay, C. W., et al. (2023). The Next Generation of Kevlar Fiber for Improved Micrometeoroid and Orbital Debris Protection. Second International Orbital Debris Conference. Houston, TX, 4-7 December.

7. Cline II, C. J., Christiansen, E. L., McCandless, R., Miller, J., Davis, B. A., Resendez, J (2024). Preliminary Experimental Investigation of Multi-Shock Shield Performance Against Meteoritic Other Lithic Projectiles. 17th Hypervelocity Impact Symposium (HVIS). Tsukuba, Japan, 8-13 September.

8. Christiansen, E. L., et al. (2009). "Handbook for designing MMOD protection." NASA Johnson Space Center, NASA/TM-2009-214785.